Heliyon 9 (2023) e18317

Contents lists available at ScienceDirect

Heliyon

journal homepage: www.cell.com/heliyon

Effects on cell cycle progression and cytoskeleton organization of five *Bothrops* spp. venoms in cell culture-based assays

Bianca Sayuri Takayasu [a,b], Sheila Silva Rodrigues [c], Carlos Eduardo Madureira Trufen [d], Glaucia Maria Machado-Santelli [b], Janice Onuki [a,c,*]

[a] *Laboratory of Structural Biology, Butantan Institute, São Paulo, Brazil*
[b] *Department of Cell and Developmental Biology, Institute of Biomedical Sciences, University of São Paulo, São Paulo, Brazil*
[c] *Laboratory of Herpetology, Butantan Institute, São Paulo, Brazil*
[d] *Czech Centre for Phenogenomics, Institute of Molecular Genetics of the Czech Academy of Sciences, Vestec, Czech Republic*

ARTICLE INFO

Keywords:
Bothrops
Venom
Cell culture
Cytotoxicity
Cytoskeleton
Cell cycle
3R principle

ABSTRACT

Snake envenomation is a neglected tropical disease. In Brazil, the *Bothrops* genus is responsible for about 86% of snakebite accidents. Despite extensive evidence of the cytotoxicity of snake venoms, the cellular and molecular mechanisms involved are not fully understood, especially regarding the effects on cell cycle progression and cytoskeleton organization. Traditionally, the effectiveness and quality control tests of venoms and antivenoms are assessed by *in vivo* assays. Despite this, there is a rising effort to develop surrogate *in vitro* models according to the 3R principle (Replacement, Reduction, and Refinement). In this study, we treated rat liver cells (BRL-3A) with venoms from five *Bothrops* species (*B. jararaca*, *B. jararacussu, B. moojeni, B. alternatus,* and *B. neuwiedi*) and analyzed cell viability and IC_{50} by MTT assay, cell cycle phases distribution by flow cytometry, and morphology and cytoskeleton alterations by immunofluorescence. In addition, we evaluated the correlation between IC_{50} and the enzymatic and biological activities of each venom. Our results indicated that *Bothrops* spp. venoms decreased the cell viability of rat liver BRL-3A cells. The rank order of potency was *B. jararacussu* > *B. moojeni* > *B. alternatus* > *B. jararaca* > *B. neuwiedi*. The mechanisms of cytotoxicity were related to microtubules and actin network disruption, but not to cell cycle arrest. No clear correlation was found between the IC_{50} and retrieved literature data of *in vitro* enzymatic and *in vivo* biological activities. This work contributed to understanding cellular and molecular mechanisms underlying the *Bothrops* spp. venom cytotoxicity, which can help to improve envenomation treatment, as well as disclose potential therapeutic properties of snake venoms.

1. Introduction

Snakebites are a problem of global concern, especially in tropical and developing countries [1], due to their potential for lethality. According to the World Health Organization (WHO), about 4.5–5.4 million people are bitten by snakes annually: with 1.8–2.7 million developing clinical illnesses and 81,000 to 138,000 dying from complications resulting from snakebite envenoming [2]. Based on this,

* Corresponding author. Laboratory of Structural Biology, Butantan Institute, São Paulo, Brazil.
E-mail address: janice.onuki@butantan.gov.br (J. Onuki).

https://doi.org/10.1016/j.heliyon.2023.e18317
Received 15 February 2023; Received in revised form 11 July 2023; Accepted 13 July 2023
Available online 19 July 2023

the WHO classified snakebites as a neglected tropical disease in 2017 and established a plan to reduce 50% of envenomation-related deaths and disabilities by 2030 [3].

Envenomation by the *Bothrops* genus is of utmost medical importance in Brazil, accounting for nearly 86% of snakebites [4]. Local symptoms include edema, hemorrhage, inflammation, and necrosis, while systemic effects include pain, coagulopathy shock, and acute renal failure [5]. The most abundant components of *Bothrops* venoms comprise snake venom metalloproteinases (SVMPs), snake venom serine proteases (SVSPs), phospholipases (PLAs), L-amino acid oxidases (LAAOs), and lectins (LECs) [6,7].

Nevertheless, the diversity of bothropic venom composition implies distinct toxic activities [7,8] associated with local and systemic envenomation effects, which are not neutralized efficiently by current serum therapy [9]. Despite the extensive evidence of snake venom's cytotoxicity [10], the underlying cellular and molecular mechanisms are not fully understood, especially regarding the effects on cell cycle progression and cytoskeleton organization.

The cell cycle progression, regulated by checkpoint proteins, consists of five phases, designated G0 (gap 0), G1 (gap 1), S (DNA synthesis), G2 (gap 2), and M (mitosis). The checkpoint proteins monitor not only the integrity of cellular components but also the fidelity of DNA synthesis [11]. The dysregulation of these checkpoints is an effective way to induce cell cycle arrest and prevent cell proliferation used by several cytotoxic agents [12]. Arresting in the G0/G1 or G2/M phases could lead to cell inhibition, ultimately resulting in cell death [13].

The cytoskeleton, composed of microtubules, actin microfilaments, and intermediate filaments, plays a crucial role in various cellular functions. Microtubules, made of α and β-tubulin dimers, are involved in mitotic spindle assembly, intracellular transport, organelle positioning, cell-cell signaling, motility, and cell morphology maintenance [14]. Actin microfilaments are F-actin-based linear double helical structures that participate in cell morphogenesis, membrane dynamics, cell mechanics, gene transcription, and protein translation [14]. Many cytotoxic compounds can bind to microtubules, modifying their polymerization and dynamics, leading to mitosis blocking and cell death [15]; a disorganized actin network is related to loss of cell adhesion, migration, and metastasis [16], actin machinery is closely involved in the programmed cell death [17], and actin cytoskeleton also plays an essential role in virus infection [18] and immune response [19].

Traditionally, the effectiveness and quality control tests of venoms and antivenoms are assessed by *in vivo* assays [20]. Despite this, there is a rising effort to develop surrogate *in vitro* models [21] according to the 3R principle (Replacement, Reduction, and Refinement) [22,23]. The Replacement principle encourages the development of alternative methods, such as *in vitro* or *in silico* tests, to reduce reliance on animal testing. The Reduction principle aims to minimize the number of animals in the experimental designs, enhancing techniques to avoid waste and integrating *in vivo* with *in vitro* and *ex vivo* techniques at different research stages. The Refinement principle values the animal's welfare, seeking to avoid unnecessary risks and reduce suffering during experimental conditions [24].

In this study, we investigated the effects of five *Bothrops* spp. venoms on cell viability, distribution of cell cycle phases, cell morphology, and cytoskeleton organization. Besides, we evaluated the correlation between the venom concentration able to reduce 50% of cell viability (IC_{50}) and *in vitro* enzymatic or *in vivo* biological activities to propose this cell culture model as an alternative method that complies with the principle of the 3Rs.

Our results indicated that *Bothrops* spp. venoms decreased the cell viability of rat liver BRL-3A cells. The rank order of potency was *B. jararacussu* > *B. moojeni* > *B. alternatus* > *B. jararaca* > *B. neuwiedi*. The mechanisms of cytotoxicity seem to be related to microtubules and actin network disruption, but not to cell cycle arrest. No clear correlation was found between the IC_{50} and enzymatic or biological activities.

2. Methods

2.1. Bothrops spp. venoms

We used the venoms from five *Bothrops* species (*B. jararaca, B. jararacussu, B. moojeni, B. alternatus, and B. neuwiedi)*. Each venom was collected separately from specimens maintained at the Laboratory of Herpetology of Butantan Institute, pooled, snap-frozen, lyophilized, and stored at −20 °C. Before use, each venom was reconstituted in sterile phosphate saline buffer at 1 mg/mL, sterilized by 0.22 μm syringe filtration, and stored at −20 °C in aliquots, which were thawed and diluted just before use. The same venom lot (01/19-1) was used for all the experiments.

2.2. Cell culture

Human retinal pigment epithelial cells (RPE-1, CRL-4000 ATCC, USA) and rat immortalized liver cells (BRL-3A, BCRJ, Brazil) were cultivated in DMEM-F12 culture medium (GIBCO, USA) with fetal bovine serum supplementation (10%) and antibiotics penicillin (100 IU/mL) and streptomycin (0.1 mg/mL) at 37 °C with 5% CO_2.

2.3. Treatment of cells with Bothrops spp. venoms

2.3.1. Cell viability and calculation of IC_{50}

For cell viability assay and calculation of the IC_{50}, 1.5×10^4 cells of RPE-1 or 5×10^3 cells of BRL-3A were seeded in a 96-well plate and incubated at 37 °C with 5% CO_2 for 16 h before treatment with *Bothrops* spp. venoms in a DMEM-F12 medium without fetal bovine serum supplementation for 24 h at 37 °C with 5% CO_2. Each venom (1 mg/mL) was diluted to concentrations from 0.5 to 10 μg/mL in

DMEM-F12 medium, and 100 μL was added to each well. DMEM-F12 alone was used as a control sample. After treatment, the medium was removed, 100 μL of the MTT solution (1.0 mg/mL) was transferred to each well and the plate was incubated at 37 °C for 4 h. The MTT solution was removed and 100 μL of DMSO was added to each well, placed at 37 °C for 5 min, and absorbance at 570 nm and 630 nm were read in BioTek's Gen5™ Data Analysis software [25]. The absorbance values at 630 nm were subtracted from the values at 570 nm and the percentage of cell viability was calculated relative to the control (set as 100%) by the mean ± SD or SEM of three independent experiments with six replicates for each sample [25]. The IC_{50} values were calculated using the functions drm and ED from the R package for "Analysis of Dose-Response Curves", dcr [26]. The corresponding figure was plotted using ggplot2 [27]. Statistical analysis was performed using Dunnett's test - ANOVA.

2.3.2. *Correlation of IC_{50} and enzymatic and biological activities of Bothrops spp. venoms*

To evaluate the correlation between IC_{50} and the enzymatic and biological activities of each venom, we retrieved data on phospholipase A_2, hyaluronidase, and proteolytic activities from Queiroz et al. (2008) [7] and hemorrhagic, necrotizing, edematogenic, coagulant, and myotoxic activities from Ferreira et al. (1992) [8]. Both works used venoms from specimens maintained at the Laboratory of Herpetology of Butantan Institute. The medium values of the lethal dose (LD_{50}) stipulated for each venom were obtained from the technical control reports of the same venoms' lot (01/19-1) used in the experiments. In the linear regression analysis, IC_{50} was the dependent variable, and the venom activities were the independent variables. The correlation coefficient was calculated by Pearson's product-moment, using the cor.test function from the stats package in R base [28]. The strength of the correlation coefficient (R) was classified according to the correlation coefficient range: [0.0, 0.19] very weak; [0.20, 0.39] weak; [0.40, 0.59] moderate; [0.60, 0.79] strong; and [0.80–1] extraordinarily strong, considering significant a p-value <0.05.

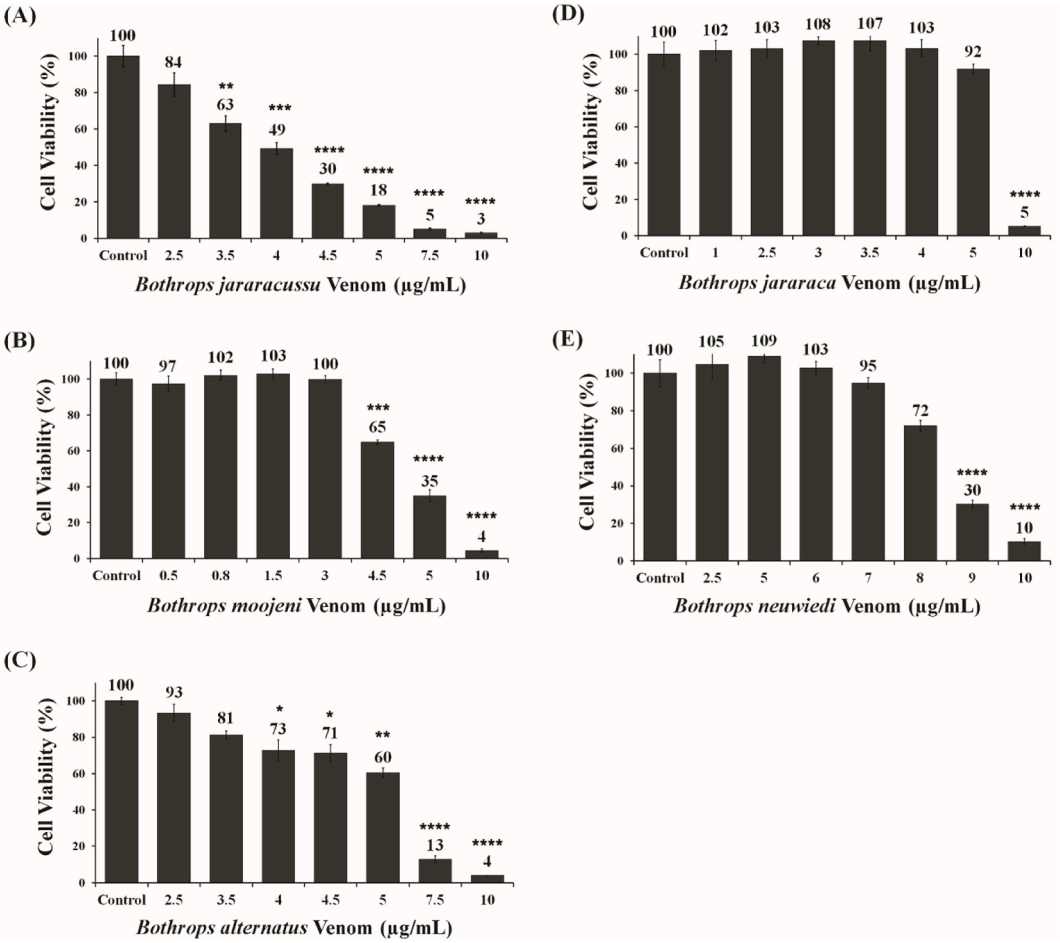

Fig. 1. Cell viability measured by MTT assay of BRL-3A cells treated with *B. jararacussu* (A), *B. moojeni* (B), *B. alternatus* (C), *B. jararaca* (D), or *B. neuwiedi* (E) venoms from 0.5 μg/mL to 10 μg/mL for 24 h. Data were expressed by mean ± SEM of the relative percentage of the control of three independent experiments with four replicates for each sample. The Dunnett - ANOVA test performed statistical analysis for multiple comparisons vs. control. (*p < 0.05, **p < 0.01, ***p < 0.001, ****p < 0.0001).

2.3.3. Cell cycle phases distribution

For analysis of the cell cycle phases distribution, BRL-3A cells (3.1×10^4 cells/well) were plated in 6-well plates, incubated for 48 h, and treated with *B. jararacussu* 3 μg/mL, *B. moojeni* 4 μg/mL, *B. alternatus* 5 μg/mL, *B. jararaca* 5.5 μg/mL or *B. neuwiedi* 7.5 μg/mL venoms in DMEM-F12 medium without fetal bovine serum supplementation for 24 h at 37 °C with 5% CO_2. DMEM-F12 alone was used as a control sample. Then, cells were fixed with cold 75% methanol at room temperature for 1 h, followed by washing with phosphate-buffered saline (PBSA). DNA was stained with propidium iodide (10 μg/mL) diluted in PBSA containing RNase (1 mg/mL) and incubated at 4 °C for 1 h. Analysis was performed on a flow cytometer (GUAVA EasyCyte Plus, MA, USA). Because the number of cells available after treatment with IC_{50} of each venom was not sufficient to obtain reliable results, we set to decrease 1 μg/mL from IC_{50} values of each venom for the cell cycle and cell morphology assays.

2.3.4. Cell morphology and nuclear and cytoskeleton analyses

Nuclear and cell morphology were analyzed by photographed images in bright field microscopy with a 20x objective (Life Technologies EVOS XL Digital Imaging System) and by immunofluorescent staining. BRL-3A cells were cultured on coverslips in 35 mm plates and treated with each *Bothrops* spp. venoms for 24 h, as described before. Cells were fixed with formaldehyde (3.7%) for 30 min and permeabilized with Triton X-100 (0.5%) for 30 min [29]. The samples were washed with PBSA, immunostained with primary monoclonal antibodies produced in mice, anti-α-tubulin (1:50) and anti-β-tubulin (1:50) (Sigma-Aldrich, MO, USA), and incubated overnight at room temperature in the dark. Corresponding secondary antibody anti-mouse IgG (H + L), $F(ab')_2$ Fragment (Alexa Fluor® 488 Conjugate) (1:50) (Cell Signaling Technology®, MA, USA), was incubated for 2 h. Actin microfilaments were labeled with phalloidin conjugated to Alexa Fluor® 555 (1:20) (Sigma-Aldrich, MO, USA) for 2 h. Nuclei were labeled with DAPI (1:100) (Sigma-Aldrich, MO, USA), and the coverslips were mounted with Vecta-Shield (Vector Laboratories, CA, USA). Analyses were performed on the LionHeart FX fluorescence microscope (Biotek, VT, USA).

3. Results

3.1. Cell viability and IC_{50}

At first, we compared the effect of *B. jararaca* venom on the cell viability in two immortalized cell lines: human retinal pigment epithelial cells (RPE-1) and rat liver cells (BRL-3A). *B. jararaca* crude venom caused morphological alterations and cytotoxicity in both cell lines (Figs. 1 and 4, S1, and S2 - Supplementary Material). The cell density of the RPE-1 line gradually decreased, forming clusters above 75 μg/mL (Fig. S1). These results were supported by a concentration-dependent decrease in cell viability, with 20 μg/mL of venom causing a significant reduction of RPE-1 cell viability (58.7 ± 6.2%), which smoothly diminished to 28.1 ± 9.1% at 75 μg/mL until 9.3 ± 2.2% at 150 μg/mL (Fig. S2). In comparison, BRL-3A cells presented morphological alterations from 5 μg/mL (Fig. 4E), with a drastic decrease in cell viability at 10 μg/mL (5.2 ± 0.3%) (Fig. 1D). The IC_{50} for RPE-1 cells was 31.7 ± 14.1 μg/mL, and the IC_{50} for BRL-3A cells was 6.6 ± 0.4 μg/mL (Fig. 2).

Given that the IC_{50} of RPE-1 cells was much higher than BRL-3A cells and most of the *in vivo* tests were first conducted in rats or mice, we selected BRL-3A rat liver cells for further investigation. Treatment of BRL-3A cells with 0.5–10 μg/mL of five *Bothrops* spp. venoms affected cell viability. In the MTT assay, all five venoms presented less than 10% of cell viability at 10 μg/mL. *B. jararacussu* and *B. alternatus* venoms induced a concentration-dependent decrease starting from 2.5 μg/mL (Fig. 1A, C), while for *B moojeni* and *B. neuwiedi,* the decrease in cell viability started from 4.5 μg/mL and 8 μg/mL respectively (Fig. 1B, E). *B. jararaca* venom presented an abrupt decrease in cell viability from 92.0 ± 4.5% with 5 μg/mL to 5.2 ± 0.3% with 10 μg/mL (Fig. 1D).

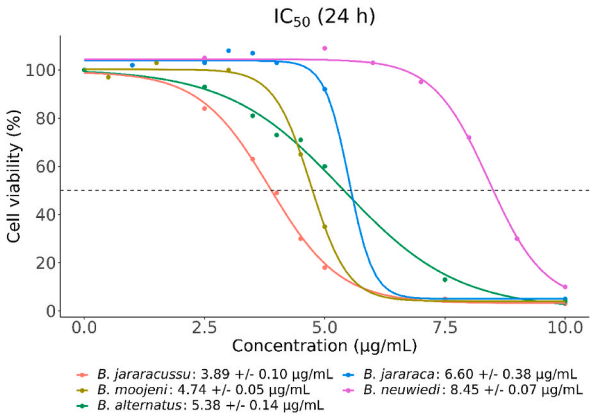

Fig. 2. Venom concentrations able to reduce 50% of cell viability (IC_{50}) of BRL-3A cells treated with *B. jararacussu*, *B. moojeni*, *B. alternatus*, *B. jararaca*, or *B. neuwiedi*, from 0.5 μg/mL to 10 μg/mL, for 24 h. Cell viability was measured by MTT assay. Data are expressed by the mean of three independent experiments with six replicates for each sample [25]. The IC_{50} values were calculated using the functions drm and ED from the dcr package [26] and were plotted using ggplot2 [27].

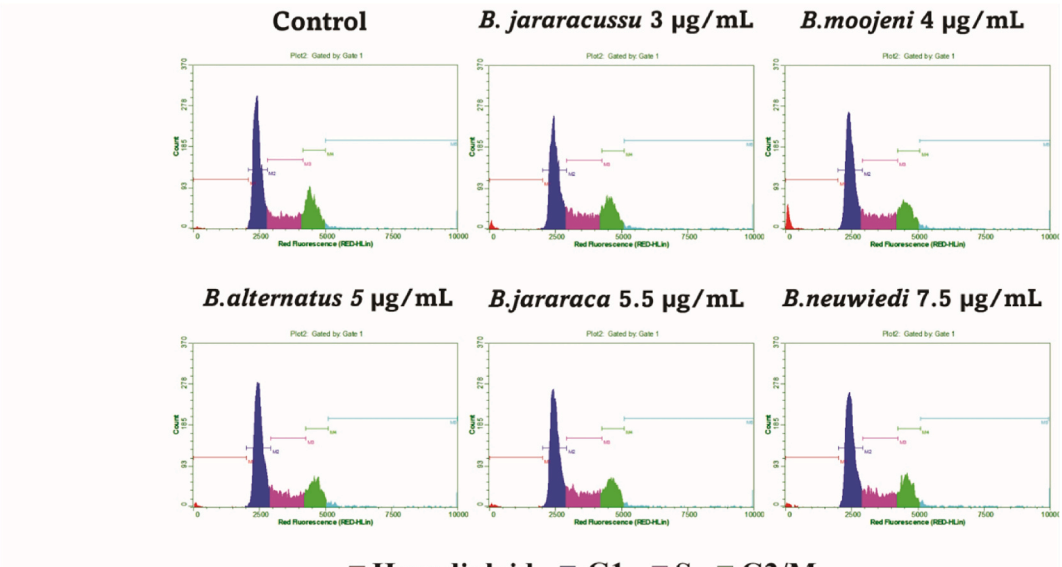

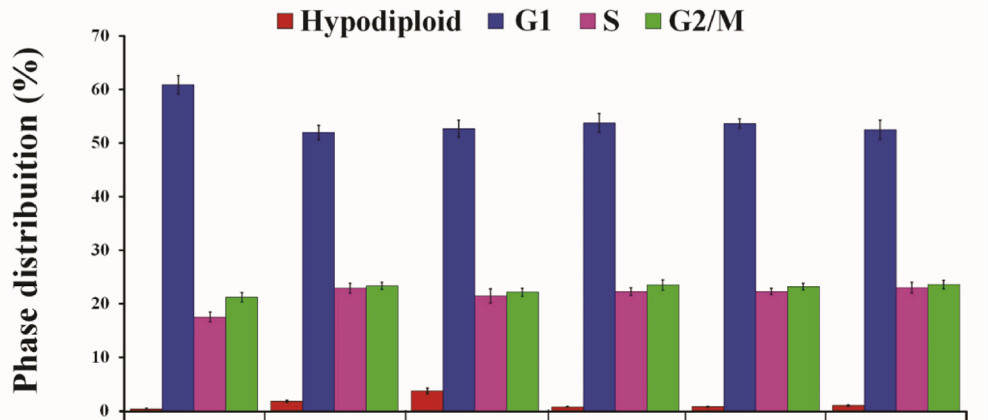

Phase	Control	*B.jararacussu* 3 µg/mL	*B.moojeni* 4 µg/mL	*B.alternatus* 5 µg/mL	*B.jararaca* 5.5 µg/mL	*B.neuwiedi* 7.5 µg/mL
Hypodiploid	0.43 ± 0.11 %	1.82 ± 0.14 %	3.75 ± 0.30 %	0.77 ± 1.62 %	0.80 ± 0.54 %	0.98 ± 0.15 %
G1	60.89 ± 5.23 %	51.95 ± 2.63 %	52.67 ± 5.37%	53.77 ± 4.71 %	53.69 ± 4.16 %	52.46 ± 5.34 %
S	17.49 ± 2.76 %	22.89 ± 1.70 %	21.47 ± 3.10 %	22.25 ± 4.03 %	22.26 ± 2.80 %	22.98 ± 2.20 %
G2/M	21.20 ± 2.73 %	23.34 ± 1.89 %	22.12 ± 2.43 %	23.46 ± 2.28 %	23.24 ± 2.08 %	23.58 ± 2.85%

Fig. 3. Flow cytometry distribution of cell cycle phases of BRL-3A cells treated with *B. jararacussu* 3 µg/mL, *B. moojeni* 4 µg/mL, *B. alternatus* 5 µg/mL, *B. jararaca* 5.5 µg/mL or *B. neuwiedi* 7.5 µg/mL for 24 h. Hypertetraploid cells were not included in the construction of the histogram. Data were expressed by mean ± SEM of the relative percentage of the control of three independent experiments with two replicates for each sample.

BRL-3A cell line presented the following IC_{50} for each venom: *B. jararacussu* (3.9 ± 0.1 µg/mL), *B. moojeni* (4.7 ± 0.05 µg/mL), *B. alternatus* (5.4 ± 0.1 µg/mL), *B. jararaca* (6.6 ± 0.4 µg/mL), and *B. neuwiedi* (8.4 ± 0.1 µg/mL) (Fig. 2).

One of the limitations of this experiment is that the cell viability evaluated by MTT assay is an indirect measurement of an integrated set of enzyme activities that are related in many ways to cell metabolism rather than a direct cell count [30].

3.2. Correlation of IC_{50} and enzymatic and biological activities of Bothrops spp. venoms

To evaluate if toxicity analysis in BRL-3A cell culture might be eligible as a surrogate *in vitro* model according to the 3R principle, we calculated the correlation coefficient R of the IC_{50} obtained in cell viability assay with previous *in vitro* enzymatic activities, the medium lethal dose (LD_{50}), and biological activities in mice [7]. We plotted the linear regression of each comparison and calculated the

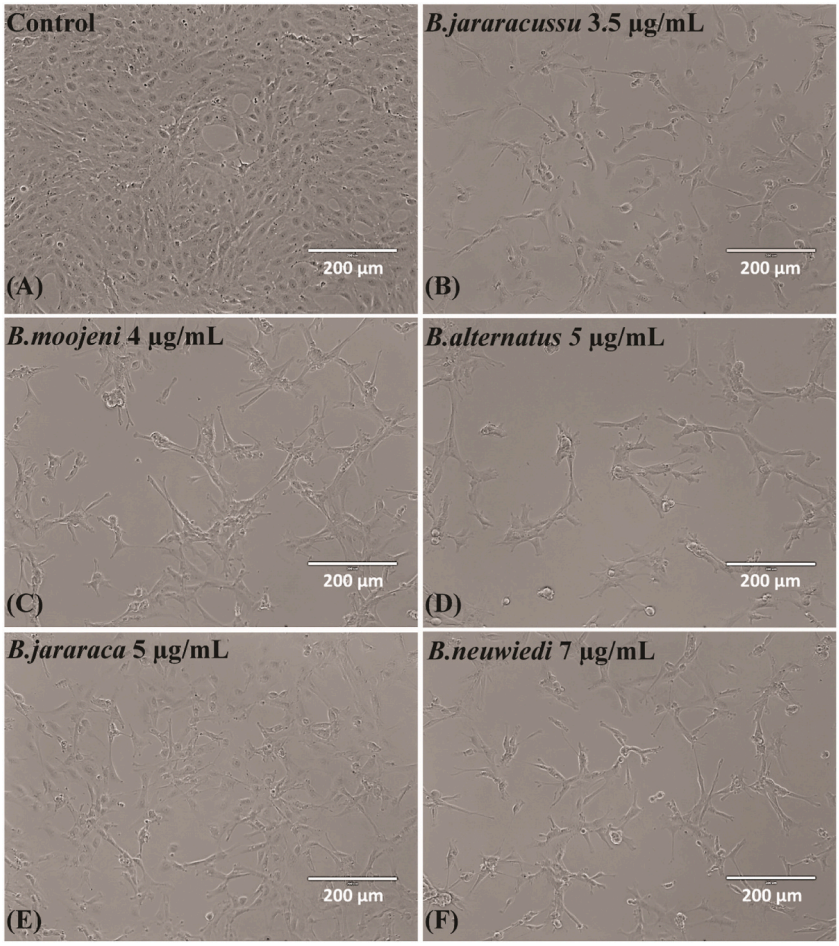

Fig. 4. Cell morphology after treatment of BRL-3A cells with Control (A), *B. jararacussu* 3.5 µg/mL (B), *B. moojeni* 4 µg/mL (C), *B. alternatus* 5 µg/mL (D), *B. jararaca* 5 µg/mL (E), or *B. neuwiedi* 7 µg/mL (F) for 24 h. Bar = 200 µm.

correlation coefficient R (Table 1).

No clear correlation could be calculated between the IC_{50} values and LD_{50} values retrieved from the Lot report (−0.73) and Queiroz et al., 2008 (−0.78). Regarding enzymatic activities, a moderate correlation between IC_{50} and hyaluronidase activity (0.27), or

Table 1
Results of Pearson's product-moment correlation coefficient between IC_{50} X enzymatic activities and biological activities of five *Bothrops* spp. venoms.

Venom activity	R	statistic	p.value	conf.low	conf.high
Lethal					
LD_{50} a (mg/kg)	−0.78	−2.13	0.12	−0.98	0.34
LD_{50}-Lot (µg/animal)	−0.73	−1.84	0.16	−0.98	0.43
Enzymatic					
PLA_2 a (nmol/min/mg)	−0.31	−0.56	0.61	−0.94	0.79
Hyal a (UTR/mg)	0.27	0.49	0.66	−0.80	0.93
Prot a (U/µg)	0.27	0.48	0.66	−0.80	0.93
Biological					
Hemo b (mm2/µg)	0.22	0.39	0.72	−0.82	0.92
Edema b (mg/µg)	0.41	0.78	0.49	−0.74	0.95
Necro b (mm2/µg)	0.84	2.70	0.07	−0.16	0.99
Myo b (U/mg)	−0.34	−0.54	0.63	−0.94	0.77
Coag b (mg-1)	0.75	1.97	0.14	−0.39	0.98

LD_{50}: medium lethal dose. LD_{50} Lot: Data from quality control report of extracted venoms (lot Bja 01/19-1) Butantan Institute. PLA_2: phospholipase A_2, HYAL: hyaluronidase, Prot: proteolytic, Hemo: hemorrhagic, Edema: edematogenic, Necro: necrotizing, Myo: myotoxic, Coag: coagulant. R: correlation coefficient; conf.low: low limit of the confidence interval; conf.high: high limit of the confidence interval. [a] Data from Queiroz et al., 2008 [7] [b] Data from Ferreira et al., 1992 [8].

proteolytic activity (0.27) was found. The correlation of IC_{50} values with biological activity values was very weak for hemorrhagic (0.22), myotoxic (−0.34), edematogenic (0.41), and coagulant (0.75) activities considering the p-value >0.05. The correlation coefficient R for necrotizing activity was 0.84 (p-value = 0.07), which suggests a potential correlation with IC_{50}. However, further

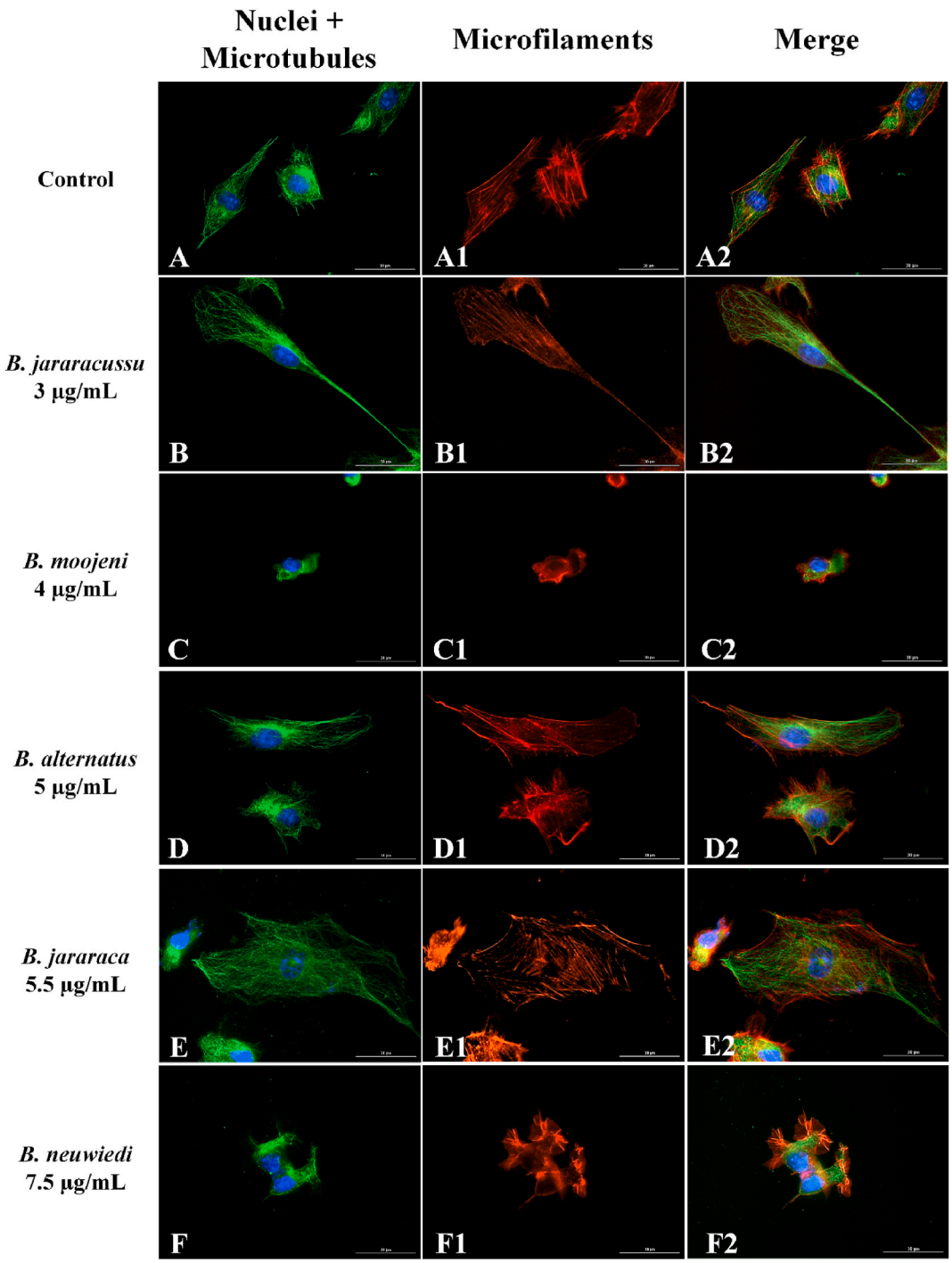

Fig. 5. Fluorescence microscopy images of BRL-3A cytoskeleton. Images of control (A) and after 24 h treatment of BRL-3A with *B. jararacussu* 3 µg/mL (B), *B. moojeni* 4 µg/mL (C), *B. alternatus* 5 µg/mL (D), *B. jararaca* 5.5 µg/mL (E) or *B. neuwiedi* 7.5 µg/mL (F), submitted to immunofluorescence reaction with antibodies against α and β-tubulin (microtubules) plus anti-mouse secondary antibodies conjugated to Alexa Fluor 488 (green). Microfilaments of F-actin were stained by phalloidin - Alexa Fluor 555 (red) and nuclei by DAPI (blue). Bar = 30 µm. (For interpretation of the references to color in this figure legend, the reader is referred to the Web version of this article.)

standardized experiments with a higher number of replicates are required for the establishment of a statistically significant correlation.

3.3. Cell cycle phases distribution

To deeply investigate the mechanism of action of cytotoxicity induced by each venom, we analyzed the cell cycle phases distribution of treated BRL-3A cells (Fig. 3). All the venoms' treatments resulted in quite a similar cell distribution. Compared with the control, the hypodiploid, S, and G2/M phases presented a slight increase with a decrease in the G1 phase. The frequency of hypertetraploid corresponds to cells with a DNA ploidy of more than 4 N, which do not belong to any specific cell cycle phase. Therefore, they were not considered to calculate the frequencies of the G1, S, and G2/M populations (Fig. 3). However, the inclusion of hypertetraploid cells in the calculation resulted in a frequency ranging from 3.52 ± 0.55% to 3.86 ± 0.70% (Fig. S4). Since this assay is based on the DNA staining according to the different cell ploidy along the cell cycle phases, it was not possible to determine if the cells continue cycling or can proliferate.

3.4. Cell morphology and nuclear and cytoskeleton analyses

Analysis of bright field images of BRL-3A cells acquired in the cell viability assay showed that all the venoms caused a decrease in cell density and altered cell morphology (Fig. 4A–F). These results prompted us to verify the presence of alterations in the nucleus and cytoskeleton by immunofluorescent staining of microtubules and actin microfilaments (Figs. S3 and 5A–F).

In the panel of Fig. 5A–F, we showed representative fluorescent images with the nucleus in blue, α and β-tubulins of the microtubules in green, and F-actin microfilaments in red. No significant alteration in the nucleus morphology was observed (Fig. S3). The effect of cell shrinkage induced by *B. moojeni* (Fig. 5C, C1, C2) and *B. neuwiedi* (Fig. 5F, F1, F2) venoms was similar. *B. jararacussu's* venom induced spindle-shaped cells (Fig. 5B, B1, B2). On the contrary, *B alternatus* venom presented the least affected cell morphology (Fig. 5D, D1, D2). Oddly, *B. jararaca* venom induced the formation of giant cells (Fig. 5E, E1, E2).

4. Discussion

The cytotoxicity of snake venoms has long been known [31]. However, different cell lines exhibit significant variations in venom susceptibility. We selected the BRL-3A cell line from rat liver to assess the toxicities of *Bothrops* spp. venoms because it is well characterized *in vitro* [32]. Our results showed that BRL-3A cells were more susceptible to *B. jararaca* venom than RPE-1 cells, with an IC_{50} of 6.6 ± 0.4 μg/mL, compared to RPE-1 (31.7 ± 14.1 μg/mL). Other studies showed an IC_{50} of 11.79 μg/mL in Vero cells [33] and an IC_{50} of 9.96 μg/mL in MGSO-3 cells [34], suggesting that the BRL-3A cell line, a non-tumoral rat liver cell, is more susceptible than the human mammary tumor cell line MGSO-3 and the Vero monkey kidney cell line.

In MGSO-3 cells, the rank order of potency of bothropic venoms and IC_{50} (μg/mL) are *B. neuwiedi* (4.07) > *B. jararacussu* (4.24) > *B. moojeni* (4.66) > *B. jararaca* (9.96)> *B. alternatus* (12.42) [34]. Our results showed the following rank order of potency and IC_{50} (μg/mL) for BRL-3A cells: *B. jararacussu* (3.9 ± 0.1 μg/mL), *B. moojeni* (4.7 ± 0.05 μg/mL), *B. alternatus* (5.4 ± 0.1 μg/mL), *B. jararaca* (6.6 ± 0.4 μg/mL), and *B. neuwiedi* (8.4 ± 0.1 μg/mL) (Fig. 2). Comparing the rank order of IC_{50} of the MGSO-3 and BRL-3A cell lines, it is interesting to note that the IC_{50} of *B. neuwiedi* was the lowest for the MGSO-3 but highest for the BRL-3A line. For other venoms, the order of IC_{50} was almost the same. However, comparisons of IC_{50} and LD_{50} values of each venom from the same lot used in all the experiments showed a different susceptibility pattern. The rank order of potency and LD_{50} (μg/animal) was *B. neuwiedi* (31.26) > *B. jararaca* (48.71) > *B. jararacussu* (82.38) > *B. alternatus* (126.38) > *B. moojeni* (131.08).

Even if *in vivo* testing cannot be completely replaced, cell culture offers an alternative to the widespread use of animal models. Although BRL-3A cell culture is a well-characterized model for *in vitro* toxicity assays [35], the liver is not an organ usually affected by envenomation, which could explain the lack of correlation between IC_{50} and enzymatic or biological activities of *Bothrops* spp. venoms, especially with LD_{50} (Table 1). Despite this, other cell lines and viability assays have already been proposed as a surrogate *in vitro* model to assess the toxic effect of venoms and antivenoms [36]. In the human primary breast cancer MGSO-3 cell line, the IC_{50} *of Bothrops* spp. *venoms*, measured by neutral red incorporation, showed no correlation with LD_{50} but presented positive correlations with LAAO activity, necrosis, and edema [34]. On the other hand, a positive correlation was found in Vero cells between IC_{50} and LD_{50} of some species of the *Bothrops* genus [37]. Vero cells and AlamarBlue® reagent have been proposed as viable alternatives for determining bothropic antivenom potency [33]. In addition to cell culture, alternative *in vitro* assays have also been under development, such as the *Artemia salina* bioassay as a potential surrogate test of dermonecrosis in mice [38] and embryonated eggs to assess antivenom potency [39].

For an effective establishment of any surrogate model for *in vivo* assays, the inherent complexity of venoms should be considered, their inter and intraspecies differences [40], the need for a strong correlation between *in vitro* and *in vivo* tests, and the intrinsic variation of each *in vitro* model. Even considering the requirement of systematic correlation analysis with a high number of replicates, cell culture with viability assays still represents a valuable alternative to pursue the reduction and refinement of animal use according to the 3R principle.

Snake venoms are a complex mixture of molecules, including snake venom metalloproteinases (SVMPs), snake venom serine proteases (SVSPs), hyaluronidases (HYALs), phospholipases (PLAs), L-amino acid oxidases (LAAOs), lectins (LECs), and others [41], each with a unique mechanism of action that reflects the diversity of biological effects related to the envenomation clinical manifestations [7,8].

In general, SVMPs are associated with hemorrhage due to direct action on specific components of the microvasculature [42], which

contributes significantly to envenomation lethality [5]. SVSPs are toxins that affect platelet aggregation, several factors of the coagulation cascade, and fibrinolytic and kallikrein-kinin systems activity, which have been associated with the hemostatic disorders of envenomation [43]. PLAs hydrolyze membrane phospholipids, generating arachidonic acid, the precursor of leukotrienes and prostaglandins, involved in numerous homeostatic biological functions, vascular permeability, and inflammation [44]. LAAOs exert actions on platelet aggregation, induction of apoptosis, hemorrhage, and cytotoxicity [45]. LECs are haemotoxic, and can be anticoagulant, platelet aggregation inhibitors, or platelet aggregation agonists [46].

Besides systemic effects, envenomation by bothropic venoms induces several local damages, such as edema, pain, and tissue necrosis [47]. SVMPs and PLAs are central in edema [48,49] and hyperalgesic effects [50]. Myonecrosis resulted from a direct action of PLAs on the cell membrane, vascular alterations caused by SVMPs, LAAOs interaction with the cell surface and internalization, or ionic status disturbances controlled by other proteins [47,51].

Analyzing the venom's effects on cell cycle progression, we observed that the cell cycle phases distribution showed a slight increase in the number of cells in hypodiploid, S, and G2/M phases with a decrease in the G1 phase, suggesting that modulation of the cell cycle may not be the leading mechanism of action of none of the *Bothrops* spp. venoms.

The observed reduction of cell density (Fig. 4A–F) upon incubation with the bothropic venoms might be due to a loss of cell adhesion and probably to some type of cell death, such as necrosis, apoptosis, autophagia or others [52], which have already been proposed as mechanisms of cell death of some *Bothrops* spp. venoms and toxins [51,53,54]. BthTX-II, a PLA_2 from *B. jararacussu* venom, causes no alteration in the cell cycle phase distribution of MCF10A breast epithelial cells but inhibits cell proliferation and promotes G2/M cell cycle arrest in MDA-MB-231 breast cancer cells [55]. Treatment of tumoral cell lines with BthTX-I, another PLA_2 from *B. jararacussu* venom, promotes G0/G1 cell cycle arrest and apoptosis [56,57]. *B. jararaca* and *B. erythromelas* snake venoms promote G0/G1 cell cycle arrest, nuclear condensation, fragmentation, and induce apoptosis via mitochondrial depolarization in cervical cancer cells [53]. LAAO from *B. atrox* snake venom triggers apoptosis, necrosis, and autophagy in normal human keratinocytes [51].

Each venom caused remarkable but distinct morphological changes through cytoskeleton disruption (Fig. 5A–F). *B. jararacussu's* venom induced spindle-shaped cells with thin protrusions (Fig. 5B, B1, B2). Microtubules were more affected than actin microfilaments with *B. moojeni* (Fig. 5C, C1, C2) and *B. neuwiedi* (Fig. 5F, F1, F2) venoms, which induced cell shrinkage, microfilament aggregates and loss of cell adhesion. *B. alternatus* venom had a lesser impact on cell morphology (Fig. 5D, D1, D2), displaying a cytoskeleton network similar to the control cells (Fig. 5A, A1, A2). Notably, *B. jararaca* venom induced an abnormal microtubule organization, leading to the formation of mononucleated giant cells (Fig. 5E, E1, E2).

Histopathological analysis of muscle from chick biventer cervicis treated with different bothropic venoms shows myonecrosis, characterized by the disorganization of myofibrils with subsequent digestion of the myofilaments, condensation of nuclear chromatin with a decrease in volume and dislocation from its original position. Among the venoms tested, *B. jararacussu* venom caused the greatest extent of myonecrosis, followed by *B. moojeni*, *B. neuwiedi*, and *B. jararaca* [58]. Comparative analysis of local effects caused by *B. alternatus* and *B. moojeni* snake venoms demonstrated that the myotoxicity caused by *B. moojeni* venom is more prominent than *B. alternatus* venom [48]. Consistent with these findings, our results indicated that *B. jararacussu, B. moojeni*, and *B. neuwiedi* venoms induced a high extent of cytoskeleton alterations, followed by *B. jararaca* and *B. alternatus* (Fig. 5A–F).

Comparing the venom composition of *Bothrops* spp., SVMPs are found to be the most abundant component [7]. In *B. jararacussu* venom, PLAs equally contribute to venom composition as SVMPs followed by LAAOs, SVSPs, and LECs. In *B. moojeni* venom, PLAs and SVSPs are the second most abundant components, followed by LAAOs/LECs. *B. neuwiedi* venom presents LAAOs as the second most abundant component, followed by equal contributions of PLAs, SVSPs, and LECs. SVMPs contribute to almost 50% of the venom composition of *B. alternatus*, followed by LAAOs/LECs, and PLAs/SVSPs. SVMPs and SVSPs contribute equally to *B. jararaca* venom, followed by PLAs and LAAOs/LECs, reviewed by Mamede et al., 2020 [5].

PLA_2 and its active phosphorylated form were shown to relocate at protrusions of the cell membrane involved in actin and membrane dynamics [59]. Arachidonic acid produced by PLAs induces actin polymerization and bundling, affecting cytoskeleton and cell morphology [60]. PLA_2 can hydrolyze phospholipids, altering plasma membrane microviscosity, which disturbs actin dynamics and cell motility [61]. Furthermore, the permeabilization and disruption of the cell membrane integrity catalyzed by PLA_2 result in an uncontrolled influx of extracellular molecules, such as Ca^{2+} ions, which trigger a set of events that lead to cell death [62,63]. In addition, the reaction catalyzed by PLA_2s releases free fatty acids, such as arachidonic acid and lysophospholipids, which are precursors for several signaling molecules involved in inflammatory processes and pain [64–67].

BJcuL, a lectin derived from *B. jararacussu* venom, induces apoptosis and actin cytoskeleton disassembly in gastric tumoral cells [54] and affects the adhesion and growth of the tumor and endothelial cells [68]. In lung cancer cells, Daboialectin, a lectin from *Daboia russelli* venom, produces morphological changes, including a spindle-like shape leading to loss of cell-cell contact [69]. *B. moojeni* crude venom disrupts the integrity of F-actin-rings in osteoclasts, which can affect their bone resorption capacity [70].

Therefore, the interspecific variation in the venom composition and toxins properties of *Bothrops* species [7,8] might be associated with the cytotoxicity and diverse morphological alterations observed in BRL-3A cells.

Considering the complexity of the pathogenesis of envenomation, we hypothesized further putative cellular and molecular mechanisms of action, which might be synergistically associated with the venom-induced biological effects.

The mononucleated giant cells induced by *B. jararaca* venom could be originated from endoreduplication of DNA, endomitosis and nuclear fusion, failures in cytokinesis [71,72], and hepatocyte hypertrophy [73]. During development, life, and aging, hepatocytes can be mononucleated or binucleated cells. However, binuclear hepatocytes assemble all condensed chromosomes from two nuclei during mitosis, producing two mononuclear hepatocytes leading to fewer binuclear hepatocytes during liver regeneration in contrast to liver development [73]. Although it is established that proliferation is an essential process in liver regeneration, it has been shown that the liver regenerates from 30% hepatectomy by hypertrophy without proliferation, and in a 70% hepatectomy, both processes equally

account for liver regeneration [73]. It is hypothesized that hypertrophy might respond more efficiently to the immediate requirement to maintain homeostasis during regeneration and may be a general mechanism to compensate for the partial loss of the organ [73].

Besides, alterations in the cytoskeletal organization can also suggest that the activities of the Rho family of guanosine triphosphatases (RhoGTPases) may be altered by bothropic venoms, especially by *B. jararacussu* and *B. neuwiedi* venoms (Fig. 5B2 and 5F2).

RhoGTPases act as molecular switches that coordinate cytoskeletal organization and rearrangements by cycling between an active GTP-bound state, regulated by guanine nucleotide exchange factors (GEFs) [74] and an inactive GDP-bound state, stimulated by GTPase-activating proteins (GAPs) [75]. In addition, guanine nucleotide dissociation inhibitors (GDIs) may block spontaneous activation [76].

The activation or inhibition of RhoGTPases (Rho, Rac, and Cdc42) by different stimuli affects signal transduction pathways that promote formation (actin polymerization) and organization (filament bundling) of actin filaments leading to protrusions and retractions, forming lamellipodia, filopodia, and membrane ruffling [77,78]. In addition, RhoGTPases can affect microtubule dynamics, regulating the assembly and disassembly of microtubule plus end-binding proteins [79]. Therefore, RhoGTPases play a significant role in several cellular processes, such as cell morphology, motility, mitosis, proliferation, adhesion, spreading, polarity, and migration [80].

B. jararacussu impaired retracting cell rear while making a large lamellipodium in the front (Fig. 5B2). This phenotype is commonly observed upon reduced Rho activity and/or increased relative Rac activity [80]. Cellular adhesion properties seemed to be more affected by *B. neuwiedi* venom (Fig. 5F2).

Actually, Jararhagin, a metalloproteinase isolated from the venom of *B. jararaca* [81], stimulates spreading, actin dynamics, and neurite outgrowth in neuroblastoma cells through the translocation of the Rac1 to the membrane fraction, suggesting its activation [82]. Russell's viper venom (RVV) induces morphological changes in human lung cancer cells A549 through modulation of Rac, Rho, and Cdc42 expression, which affects cellular-nuclear architecture related to cell proliferation, migration, and apoptosis [83]. Furthermore, a snake c-type lectin isolated from RVV, Daboialectin, alters the morphology of A549 cells via regulation of the cytoskeleton through RhoGTPases [69]. *C. durissus terrificus* venom and its main toxin, crotoxin, cause reorganization of the actin cytoskeleton in macrophages, and crotoxin significantly reduces membrane-associated RhoA and Rac1, negatively regulating the activity of RhoGTPases [84].

In addition to actin cytoskeleton modulation, RhoGTPases regulate cell cycle progression by acting in G1/S transition, progression of mitosis, and during cytokinesis [85].

It is tempting to suggest a potential involvement of reactive oxygen species (ROS) in the observed cytoskeleton alterations. Snake venoms PLA_2 and LAAOs can generate ROS (for review see Ref. [86]), which have been associated with reduction/oxidation modifications of cysteine and methionine residues of actin, actin-binding proteins, adhesion molecules, and signaling proteins involved in regulation dynamics [87].

Furthermore, the cytoskeletal disruption without cell cycle arrest induced by *Bothrops* spp. venoms could raise a question about how actin cytoskeleton dynamics relate to cell cycle progression control [85].

Along with growth factors and adhesion to extracellular matrix (ECM), the organization of the actin cytoskeleton has been implicated in cell cycle progression since disruption of the actin network by several drugs can lead to G1 arrest in a variety of cell lines [85,88].

In normal human fibroblasts, an organized cytoskeleton rather than cell adhesion *per se* is required to promote cell cycle progression through G1 [89]. Disruption of the actin network, inhibition of cell spreading, as well as signals provided by ECM, can block the cell cycle in the G1/S transition [89].

However, other studies demonstrated that inhibition of actin assembly can result in G1 arrest without interference in cell spreading, formation of focal adhesions, or normal cellular cleavage [90]. In addition, post-mitotic disruption of the actin cytoskeleton allows cell cycle progression independently of focal adhesion signaling, cytoskeletal organization, and cell shape, presumably because pre-existing cyclin D level is sufficient to drive cell cycle progression at the M-G1 border [91]. Cell cycle progression of cycling cells with disrupted cytoskeleton depends on MAPK activity, which allows cell proliferation independently of actin stress fibers, focal adhesions, or cell spreading [92]. Therefore, it is suggested that the integrity of the actin cytoskeleton and cell spreading is required for the cell cycle progression of quiescent cells (G0), but not for cells that are already in the cycle (M-G1 cells) [92]. Likewise, the lack of alteration in the cell cycle phases distribution in our results might suggest that the cells could be able to cycle and proliferate, even if cell spreading and actin organization were strongly perturbed.

In conclusion, our results indicated that *Bothrops* spp. venoms decreased cell viability of rat liver BRL-3A cells, without cell cycle arrest. No clear correlation was found between the IC_{50} and enzymatic or biological activities. Each venom induced remarkable but distinct morphological changes through microtubules and actin network disruption, reflecting the diversity of venom composition and related physiopathological effects.

This work contributed to understanding cellular and molecular mechanisms underlying the *Bothrops* spp. venom cytotoxicity, which can help to improve envenomation treatment, as well as disclose potential therapeutic properties of snake venoms.

Funding

This work was supported by the "Fundação de Amparo à Pesquisa do Estado de São Paulo (FAPESP- 2015/17177-6)"; "Conselho Nacional de Desenvolvimento Científico e Tecnológico (CNPq-316504/2021-1)"; and "Fundação Butantan". S.S.R. received fellowships from "Centro de Formação de Recursos Humanos do Sistema Único de Saúde da Secretaria de Estado da Saúde de São Paulo (CEFOR/SUS/SES/SP 586/2021)". B.S.T. received a fellowship from "Coordenação de Aperfeiçoamento de Pessoal de Nível Superior

(CAPES-88887.508742/2020-00)".

Author contribution statement

Bianca Sayuri Takayasu: Conceived and designed the experiments; Performed the experiments; Analyzed and interpreted the data; Wrote the paper.

Sheila Silva Rodrigues: Performed the experiments.

Carlos Eduardo Madureira Trufen: Performed the experiments; Analyzed and interpreted the data; Contributed reagents, materials, analysis tools or data; Wrote the paper.

Glaucia Maria Machado-Santelli, Janice Onuki: Conceived and designed the experiments; Analyzed and interpreted the data; Contributed reagents, materials, analysis tools or data; Wrote the paper.

Declaration of competing interest

The authors declare that they have no known competing financial interests or personal relationships that could have appeared to influence the work reported in this paper.

Acknowledgments

The authors are grateful to Dra. Marisa Maria Teixeira da Rocha, who helped in the initial draft of the Material and Methods and promptly provided us with the stocked venoms and the respective control reports. We are also grateful to all the personnel of the Laboratory of Herpetology of Butantan Institute responsible for the maintenance of the indoor serpentarium and venom extraction, and the personnel of the Rodents Animal Facility at Butantan Institute for breeding and maintaining the prey used for feeding the snakes.

Appendix A. Supplementary data

Supplementary data to this article can be found online at https://doi.org/10.1016/j.heliyon.2023.e18317.

References

[1] J. Longbottom, F.M. Shearer, M. Devine, G. Alcoba, F. Chappuis, D.J. Weiss, S.E. Ray, N. Ray, D.A. Warrell, R. Ruiz de Castañeda, D.J. Williams, S.I. Hay, D. M. Pigott, Vulnerability to snakebite envenoming: a global mapping of hotspots, Lancet 392 (2018) 673–684, https://doi.org/10.1016/S0140-6736(18)31224-8.

[2] WHO Team - Control of Neglected Diseases, Snakebite Envenoming: a Strategy for Prevention and Control, WHO, 2019.

[3] WHO - Departmental News, Snakebite, WHO Targets 50% Reduction in Deaths and Disabilities, WHO, 2019. https://www.who.int/news-room/detail/06-05-2019-snakebite-who-targets-50-reduction-in-deaths-and-disabilities.

[4] R.R. Matos, E. Ignotti, Incidence of venomous snakebite accidents by snake species in brazilian biomes, Ciência Saúde Coletiva 25 (2020) 2837–2846, https://doi.org/10.1590/1413-81232020257.31462018.

[5] C.C.N. Mamede, B.B. de Sousa Simamoto, D.F. da Cunha Pereira, J. de Oliveira Costa, M.S.M. Ribeiro, F. de Oliveira, Edema, hyperalgesia and myonecrosis induced by Brazilian bothropic venoms: overview of the last decade, Toxicon 187 (2020) 10–18, https://doi.org/10.1016/j.toxicon.2020.08.016.

[6] D.D. Almeida, V.L. Viala, P.G. Nachtigall, M. Broe, H. Lisle Gibbs, S.M. De Toledo Serrano, A.M. Moura-Da-Silva, P.L. Ho, M.Y. Nishiyama, I.L.M. Junqueira-De-Azevedo, Tracking the recruitment and evolution of snake toxins using the evolutionary context provided by the Bothrops jararaca genome, Proc. Natl. Acad. Sci. U. S. A. 118 (2021) 1–10, https://doi.org/10.1073/pnas.2015159118.

[7] G.P. Queiroz, L.A. Pessoa, F.C. V Portaro, M. de Fátima D. Furtado, D. V Tambourgi, Interspecific variation in venom composition and toxicity of Brazilian snakes from Bothrops genus, Toxicon 52 (2008) 842–851, https://doi.org/10.1016/j.toxicon.2008.10.002.

[8] M.L. Ferreira, A.M. Moura-da-Silva, F.O.S. França, J.L. Cardoso, I. Mota, Toxic activities of venoms from nine Bothrops species and their correlation with lethality and necrosis, Toxicon 30 (1992) 1603–1608, https://doi.org/10.1016/0041-0101(92)90032-Z.

[9] A. Alangode, K. Rajan, B.G. Nair, Snake antivenom: challenges and alternate approaches, Biochem. Pharmacol. 181 (2020), https://doi.org/10.1016/j.bcp.2020.114135.

[10] H.P. Chong, K.Y. Tan, C.H. Tan, Cytotoxicity of snake venoms and cytotoxins from two southeast asian cobras (Naja sumatrana, Naja kaouthia): exploration of anticancer potential, selectivity, and cell death mechanism, Front. Mol. Biosci. 11 (2020), 583587, https://doi.org/10.3389/fmolb.2020.583587.

[11] A. Panagopoulos, M. Altmeyer, The hammer and the dance of cell cycle control, Trends Biochem. Sci. 46 (2021) 301–314, https://doi.org/10.1016/j.tibs.2020.11.002.

[12] R. Visconti, R. Della Monica, D. Grieco, Cell cycle checkpoint in cancer: a therapeutically targetable double-edged sword, J. Exp. Clin. Cancer Res. 35 (2016), https://doi.org/10.1186/s13046-016-0433-9.

[13] K.G. Wiman, B. Zhivotovsky, Understanding cell cycle and cell death regulation provides novel weapons against human diseases, J. Intern. Med. 281 (2017) 483–495, https://doi.org/10.1111/joim.12609.

[14] T. Hohmann, F. Dehghani, The cytoskeleton-A complex interacting meshwork, Cells 8 (2019), https://doi.org/10.3390/cells8040362.

[15] D. Bates, A. Eastman, Microtubule destabilising agents: far more than just antimitotic anticancer drugs, Br. J. Clin. Pharmacol. 83 (2017) 255–268, https://doi.org/10.1111/bcp.13126.

[16] M. Janiszewska, M.C. Primi, T. Izard, Cell adhesion in cancer: beyond the migration of single cells, J. Biol. Chem. 295 (2020) 2495–2505, https://doi.org/10.1074/jbc.REV119.007759.

[17] L.-M. Yin, C. Campillo, C. Gourlay, J. Huang, W. Ren, W. Zhao, L. Cao, Involvement of the actin machinery in programmed cell death, Front. Cell Dev. Biol. 8 (2021), 634849, https://doi.org/10.3389/fcell.2020.634849.

[18] M. Kloc, A. Uosef, J. Wosik, J.Z. Kubiak, R.M. Ghobrial, Virus interactions with the actin cytoskeleton—what we know and do not know about SARS-CoV-2, Arch. Virol. 167 (2022) 737–749, https://doi.org/10.1007/s00705-022-05366-1.

[19] D. Acharya, R. Reis, M. Volcic, G.Q. Liu, M.K. Wang, B.S. Chia, R. Nchioua, R. Groß, J. Münch, F. Kirchhoff, K.M.J. Sparrer, M.U. Gack, Actin cytoskeleton remodeling primes RIG-I-like receptor activation, Cell 185 (2022) 3588–3602.e21, https://doi.org/10.1016/j.cell.2022.08.011.

[20] WHO, WHO guidelines for the production, control and regulation of snake antivenom immunoglobulins, Biol Aujourdhui 204 (2016) 87–91.

[21] J.M. Gutiérrez, M. Vargas, Á. Segura, M. Herrera, M. Villalta, G. Solano, A. Sánchez, C. Herrera, G. León, In vitro tests for assessing the neutralizing ability of snake antivenoms: toward the 3Rs principles, Front. Immunol. 11 (2021), https://doi.org/10.3389/fimmu.2020.617429.

[22] W.M.S. Russell, R.L. Burch, C.W. Hume, Principle of Humane Experimental Techniques, Univ Federation for Animal Welfare, 1959.

[23] J. Tannenbaum, B.T. Bennett, Russell and Burch's 3Rs then and now: the need for clarity in definition and purpose, J. Am. Assoc. Lab Anim. Sci. 54 (2015) 120–132.

[24] K.C.C. Cazarin, C.L. Corrêa, F.A.D. Zambrone, Reduction, refinement and replacement of animal use in toxicity testing: an overview, Braz. J. Pharm. Sci. 40 (2004) 289–299, https://doi.org/10.1590/s1516-93322004000300004.

[25] H. Tada, O. Shiho, K. ichi Kuroshima, M. Koyama, K. Tsukamoto, An improved colorimetric assay for interleukin 2, J. Immunol. Methods 93 (1986) 157–165, https://doi.org/10.1016/0022-1759(86)90183-3.

[26] C. Ritz, F. Baty, J.C. Streibig, D. Gerhard, Dose-response analysis using R, PLoS One 10 (2015), https://doi.org/10.1371/journal.pone.0146021.

[27] H. Wickham, ggplot2, vol. 3, Wiley Interdiscip Rev Comput Stat., 2011, pp. 180–185, https://doi.org/10.1002/wics.147.

[28] R. Core Team, R:, A language and environment for statistical computing, R Foundation for Statistical Computing, Vienna, Austria, 2013. http://www.R-project.org.

[29] B.S. Takayasu, I.R. Martins, A.M.B. Garnique, S. Miyamoto, G.M. Machado-Santelli, M. Uemi, J. Onuki, Biological effects of an oxyphytosterol generated by β-Sitosterol ozonization, Arch. Biochem. Biophys. 696 (2020), https://doi.org/10.1016/j.abb.2020.108654.

[30] M. Ghasemi, T. Turnbull, S. Sebastian, I. Kempson, The MTT assay: utility, limitations, pitfalls, and interpretation in bulk and single-cell analysis, Int. J. Mol. Sci. 22 (2021), https://doi.org/10.3390/ijms222312827.

[31] C.B. Collares-Buzato, L. de Paula Le Sueur, M.A. da Cruz-Höfling, Impairment of the cell-to-matrix adhesion and cytotoxicity induced by Bothrops moojeni snake venom in cultured renal tubular epithelia, Toxicol. Appl. Pharmacol. 181 (2002) 124–132, https://doi.org/10.1006/taap.2002.9404.

[32] A.K. Al-Asmari, H.A. Khan, R.A. Manthiri, A.A. Al-Khlaiwi, B.A. Al-Asmari, K.E. Ibrahim, Protective effects of a natural herbal compound quercetin against snake venom-induced hepatic and renal toxicities in rats, Food Chem. Toxicol. 118 (2018) 105–110, https://doi.org/10.1016/j.fct.2018.05.016.

[33] L. Lopes-de-Souza, F. Costal-Oliveira, S. Stransky, C.F. de Freitas, C. Guerra-Duarte, V.M.M. Braga, C. Chávez-Olórtegui, Development of a cell-based in vitro assay as a possible alternative for determining bothropic antivenom potency, Toxicon 170 (2019) 68–76, https://doi.org/10.1016/j.toxicon.2019.09.010.

[34] L.L. De Souza, S. Stransky, C. Guerra-duarte, A. Flor-sá, F.S. Schneider, E. Kalapothakis, C. Chávez-olórtegui, Determination of toxic activities in Bothrops spp. snake venoms using animal-free approaches: correlation between in vitro versus in vivo assays, Toxicol. Sci. 147 (2015) 458–465, https://doi.org/10.1093/toxsci/kfv140.

[35] C. Li, M. Lan, J. Lv, Y. Zhang, X. Gao, X. Gao, L. Dong, G. Luo, H. Zhang, J. Sun, Screening of the hepatotoxic components in Fructus gardeniae and their effects on rat liver BRL-3A cells, Molecules 24 (2019), https://doi.org/10.3390/molecules24213920.

[36] J.J. Hiu, M.K.K. Yap, Cytotoxicity of snake venom enzymatic toxins: phospholipase A2 and L-amino acid oxidase, Biochem. Soc. Trans. 48 (2020) 719–731, https://doi.org/10.1042/BST20200110.

[37] J.C.R. Oliveira, H.M. de Oca, M.M. Duarte, C.R. Diniz, C.L. Fortes-Dias, Toxicity of south american snake venoms measured by an in vitro cell culture assay, Toxicon 40 (2002) 321–325, https://doi.org/10.1016/S0041-0101(01)00229-X.

[38] M.O. Okumu, J.M. Mbaria, J.K. Gikunju, P.G. Mbuthia, V.O. Madadi, F.O. Ochola, M.S. Jepkorir, Artemia salina as an animal model for the preliminary evaluation of snake venom-induced toxicity, Toxicon X 12 (2021), 100082, https://doi.org/10.1016/j.toxcx.2021.100082.

[39] E.E. Verity, K. Stewart, K. Vandenberg, C. Ong, S. Rockman, Potency testing of venoms and antivenoms in embryonated eggs: an ethical alternative to animal testing, Toxins 13 (2021), https://doi.org/10.3390/toxins13040233.

[40] S.M.T. Serrano, A. Zelanis, E.S. Kitano, A.K. Tashima, Analysis of the snake venom peptidome, Methods Mol. Biol. 1719 (2018) 349–358, https://doi.org/10.1007/978-1-4939-7537-2_23.

[41] J.J. Calvete, Antivenomics and venom phenotyping: a marriage of convenience to address the performance and range of clinical use of antivenoms, Toxicon 56 (2010) 1284–1291, https://doi.org/10.1016/j.toxicon.2009.12.015.

[42] N. Jiménez, T. Escalante, J.M. Gutiérrez, A. Rucavado, Skin pathology induced by snake venom metalloproteinase: acute damage, revascularization, and re-epithelization in a mouse ear model, J. Invest. Dermatol. 128 (2008) 2421–2428, https://doi.org/10.1038/jid.2008.118.

[43] S.M.T. Serrano, R.C. Maroun, Snake venom serine proteinases: sequence homology vs. substrate specificity, a paradox to be solved, Toxicon 45 (2005) 1115–1132, https://doi.org/10.1016/j.toxicon.2005.02.020.

[44] I. Galvão, M.A. Sugimoto, J.P. Vago, M.G. Machado, L.P. Sousa, Mediators of inflammation, in: C. Riccardi, F. Levi-Schaffer, E. Tiligada (Eds.), Immunopharmacology and Inflammation, Springer International Publishing, Cham, 2018, pp. 3–32, https://doi.org/10.1007/978-3-319-77658-3_1.

[45] L.F.M. Izidoro, J.C. Sobrinho, M.M. Mendes, T.R. Costa, A.N. Grabner, V.M. Rodrigues, S.L. Da Silva, F.B. Zanchi, J.P. Zuliani, C.F.C. Fernandes, L.A. Calderon, R.G. Stábeli, A.M. Soares, Snake venom L-amino acid oxidases: trends in pharmacology and biochemistry, BioMed Res. Int. 2014 (2014), https://doi.org/10.1155/2014/196754.

[46] T. Ogawa, T. Chijiwa, N. Oda-Ueda, M. Ohno, Molecular diversity and accelerated evolution of C-type lectin-like proteins from snake venom, Toxicon 45 (2005) 1–14, https://doi.org/10.1016/j.toxicon.2004.07.028.

[47] J.M. Gutiérrez, A. Rucavado, T. Escalante, C. Herrera, J. Fernández, B. Lomonte, J.W. Fox, Unresolved issues in the understanding of the pathogenesis of local tissue damage induced by snake venoms, Toxicon 148 (2018) 123–131, https://doi.org/10.1016/J.TOXICON.2018.04.016.

[48] C.C.N. Mamede, B.B. De Sousa, D.F.D.C. Pereira, M.S. Matias, M.R. De Queiroz, N.C.G. De Morais, S.A.P.B. Vieira, L. Stanziola, F. De Oliveira, Comparative analysis of local effects caused by Bothrops alternatus and Bothrops moojeni snake venoms: enzymatic contributions and inflammatory modulations, Toxicon 117 (2016) 37–45, https://doi.org/10.1016/j.toxicon.2016.03.006.

[49] B.C. Zychar, C.S. Dale, D.S. Demarchi, L.R.C. Gonçalves, Contribution of metalloproteases, serine proteases and phospholipases A2 to the inflammatory reaction induced by Bothrops jararaca crude venom in mice, Toxicon 55 (2010) 227–234, https://doi.org/10.1016/j.toxicon.2009.07.025.

[50] V.O. Zambelli, G. Picolo, C.A.H. Fernandes, M.R.M. Fontes, Y. Cury, Secreted phospholipases A 2 from animal venoms in pain and analgesia, Toxins 9 (2017) 1–27, https://doi.org/10.3390/toxins9120406.

[51] F. Costal-Oliveira, S. Stransky, C. Guerra-Duarte, D.L.N. De Souza, D.E. Vivas-Ruiz, A. Yarlequé, E.F. Sanchez, C. Chávez-Olórtegui, V.M.M. Braga, L-amino acid oxidase from Bothrops atrox snake venom triggers autophagy, apoptosis and necrosis in normal human keratinocytes, Sci. Rep. 9 (2019), https://doi.org/10.1038/s41598-018-37435-4.

[52] L. Galluzzi, I. Vitale, S.A. Aaronson, J.M. Abrams, D. Adam, P. Agostinis, E.S. Alnemri, L. Altucci, I. Amelio, D.W. Andrews, M. Annicchiarico-Petruzzelli, A. V Antonov, E. Arama, E.H. Baehrecke, N.A. Barlev, N.G. Bazan, F. Bernassola, M.J.M. Bertrand, K. Bianchi, M. V Blagosklonny, K. Blomgren, C. Borner, P. Boya, C. Brenner, M. Campanella, E. Candi, D. Carmona-Gutierrez, F. Cecconi, F.K.M. Chan, N.S. Chandel, E.H. Cheng, J.E. Chipuk, J.A. Cidlowski, A. Ciechanover, G. M. Cohen, M. Conrad, J.R. Cubillos-Ruiz, P.E. Czabotar, V. D'Angiolella, T.M. Dawson, V.L. Dawson, V. De Laurenzi, R. De Maria, K.M. Debatin, R. J. Deberardinis, M. Deshmukh, N. Di Daniele, F. Di Virgilio, V.M. Dixit, S.J. Dixon, C.S. Duckett, B.D. Dynlacht, W.S. El-Deiry, J.W. Elrod, G.M. Fimia, S. Fulda, A.J. García-Sáez, A.D. Garg, C. Garrido, E. Gavathiotis, P. Golstein, E. Gottlieb, D.R. Green, L.A. Greene, H. Gronemeyer, A. Gross, G. Hajnoczky, J.M. Hardwick, I.S. Harris, M.O. Hengartner, C. Hetz, H. Ichijo, M. Jäättelä, B. Joseph, P.J. Jost, P.P. Juin, W.J. Kaiser, M. Karin, T. Kaufmann, O. Kepp, A. Kimchi, R.N. Kitsis, D. J. Klionsky, R.A. Knight, S. Kumar, S.W. Lee, J.J. Lemasters, B. Levine, A. Linkermann, S.A. Lipton, R.A. Lockshin, C. López-Otín, S.W. Lowe, T. Luedde, E. Lugli, M. MacFarlane, F. Madeo, M. Malewicz, W. Malorni, G. Manic, J.C. Marine, S.J. Martin, J.C. Martinou, J.P. Medema, P. Mehlen, P. Meier, S. Melino, E.A. Miao, J.D. Molkentin, U.M. Moll, C. Muñoz-Pinedo, S. Nagata, G. Nuñez, A. Oberst, M. Oren, M. Overholtzer, M. Pagano, T. Panaretakis, M. Pasparakis, J. M. Penninger, D.M. Pereira, S. Pervaiz, M.E. Peter, M. Piacentini, P. Pinton, J.H.M. Prehn, H. Puthalakath, G.A. Rabinovich, M. Rehm, R. Rizzuto, C.M. P. Rodrigues, D.C. Rubinsztein, T. Rudel, K.M. Ryan, E. Sayan, L. Scorrano, F. Shao, Y. Shi, J. Silke, H.U. Simon, A. Sistigu, B.R. Stockwell, A. Strasser, G. Szabadkai, S.W.G. Tait, D. Tang, N. Tavernarakis, A. Thorburn, Y. Tsujimoto, B. Turk, T. Vanden Berghe, P. Vandenabeele, M.G. Vander Heiden, A. Villunger,

H.W. Virgin, K.H. Vousden, D. Vucic, E.F. Wagner, H. Walczak, D. Wallach, Y. Wang, J.A. Wells, W. Wood, J. Yuan, Z. Zakeri, B. Zhivotovsky, L. Zitvogel, G. Melino, G. Kroemer, Molecular mechanisms of cell death: recommendations of the nomenclature committee on cell death 2018, Cell Death Differ. 25 (2018) 486–541, https://doi.org/10.1038/s41418-017-0012-4.

[53] E. Bernardes-Oliveira, D.L. Gomes, G.M. Palomino, K.J.S. Farias, W.D. Da Silva, H.A.O. Rocha, A.K. Gonçalves, M.D.F. Fernandes-Pedrosa, J.C.D.O. Crispim, Bothrops jararaca and Bothrops erythromelas snake venoms promote cell cycle arrest and induce apoptosis via the mitochondrial depolarization of cervical cancer cells, Evid. Bas. Comp. Alter. Med. 2016 (2016), https://doi.org/10.1155/2016/1574971.

[54] S. Nolte, D. de Castro Damasio, A.C. Baréa, J. Gomes, A. Magalhães, L.F.C.M. Zischler, P.M. Stuelp-Campelo, S.L. Elífio-Esposito, M.C. Roque-Barreira, C.A. Reis, A.N. Moreno-Amaral, BJcuL, a lectin purified from Bothrops jararacussu venom, induces apoptosis in human gastric carcinoma cells accompanied by inhibition of cell adhesion and actin cytoskeleton disassembly, Toxicon 59 (2012) 81–85, https://doi.org/10.1016/J.TOXICON.2011.10.012.

[55] F.V.P. de Vasconcelos Azevedo, M.A.P. Zóia, D.S. Lopes, S.N. Gimenes, L. Vecchi, P.T. Alves, R.S. Rodrigues, A.C.A. Silva, K.A.G. Yoneyama, L.R. Goulart, V. de Melo Rodrigues, Antitumor and antimetastatic effects of PLA2-BthTX-II from Bothrops jararacussu venom on human breast cancer cells, Int. J. Biol. Macromol. 135 (2019) 261–273, https://doi.org/10.1016/J.IJBIOMAC.2019.05.164.

[56] C.P. da Silva, T.R. Costa, R.M.A. Paiva, A.C.O. Cintra, D.L. Menaldo, L.M.G. Antunes, S. V Sampaio, Antitumor potential of the myotoxin BthTX-I from Bothrops jararacussu snake venom: evaluation of cell cycle alterations and death mechanisms induced in tumor cell lines, J. Venom. Anim. Toxins Incl. Trop. Dis. 21 (2015) 44, https://doi.org/10.1186/s40409-015-0044-5.

[57] P.H.A. Bezerra, I.M. Ferreira, B.T. Franceschi, F. Bianchini, L. Ambrósio, A.C.O. Cintra, S.V. Sampaio, F.A. De Castro, M.R. Torqueti, BthTX-I from Bothrops jararacussu induces apoptosis in human breast cancer cell lines and decreases cancer stem cell subpopulation, J. Venom. Anim. Toxins Incl. Trop. Dis. 25 (2019), https://doi.org/10.1590/1678-9199-jvatitd-2019-0010.

[58] S.R. Zamunér, M.A. Da Cruz-Höfling, A.P. Corrado, S. Hyslop, L. Rodrigues-Simioni, Comparison of the neurotoxic and myotoxic effects of Brazilian Bothrops venoms and their neutralization by commercial antivenom, Toxicon 44 (2004) 259–271, https://doi.org/10.1016/J.TOXICON.2004.05.029.

[59] M. Moes, J. Boonstra, E. Regan-Klapisz, Novel role of cPLA 2 a in membrane and actin dynamics, Cell. Mol. Life Sci. 67 (2010) 1547–1557, https://doi.org/10.1007/s00018-010-0267-0.

[60] H.L. Glenn, B.S. Jacobson, Arachidonic Acid signaling to the cytoskeleton: the role of cyclooxygenase and cyclic AMP-dependent protein kinase in actin bundling, Cytoskeleton 53 (2002) 239–250, https://doi.org/10.1002/cm.10072.

[61] P.K. Ghosh, A. Vasanji, G. Murugesan, S.J. Eppell, L.M. Graham, P.L. Fox, Membrane microviscosity regulates endothelial cell motility, Nat. Cell Biol. 28 (2002) October, https://doi.org/10.1038/ncb873.

[62] A.L. Oliveira, M.F. Viegas, S.L. Da Silva, A.M. Soares, M.J. Ramos, P.A. Fernandes, The chemistry of snake venom and its medicinal potential, Nat. Rev. Chem 6 (2022) 451–469, https://doi.org/10.1038/s41570-022-00393-7.

[63] J. Fernández, P. Caccin, G. Koster, B. Lomonte, J.M. Gutiérrez, C. Montecucco, A.D. Postle, Muscle phospholipid hydrolysis by Bothrops asper Asp49 and Lys49 phospholipase A2 myotoxins - distinct mechanisms of action, FEBS J. 280 (2013) 3878–3886, https://doi.org/10.1111/febs.12386.

[64] H. Xiao, H. Pan, K. Liao, M. Yang, C. Huang, Snake venom PLA2, a promising target for broad-spectrum antivenom drug development, BioMed Res. Int. 2017 (2017), https://doi.org/10.1155/2017/6592820.

[65] J.E. Burke, E.A. Dennis, Phospholipase A2 biochemistry, Cardiovasc. Drugs Ther. 23 (2009) 49–59, https://doi.org/10.1007/s10557-008-6132-9.

[66] R.H. Schaloske, E.A. Dennis, The phospholipase A2 superfamily and its group numbering system, Biochim. Biophys. Acta Mol. Cell Biol. Lipids 1761 (2006) 1246–1259, https://doi.org/10.1016/j.bbalip.2006.07.011.

[67] J. Castro-Amorim, A.N. de Oliveira, S.L. Da Silva, A.M. Soares, A.K. Mukherjee, M.J. Ramos, P.A. Fernandes, Catalytically active snake venom PLA2 enzymes: an overview of its elusive mechanisms of reaction, J. Med. Chem. 66 (2023) 5364–5376, https://doi.org/10.1021/acs.jmedchem.3c00097.

[68] D.D. De Carvalho, S. Schmitmeier, J.Á.C. Novello, F.S. Markland, Effect of BJcuL (a lectin from the venom of the snake Bothrops jararacussu) on adhesion and growth of tumor and endothelial cells, Toxicon 39 (2001) 1471–1476.

[69] J. Pathan, S. Mondal, A. Sarkar, D. Chakrabarty, Daboialectin, a C-type lectin from Russell's viper venom induces cytoskeletal damage and apoptosis in human lung cancer cells in vitro, Toxicon 127 (2017) 11–21, https://doi.org/10.1016/j.toxicon.2016.12.013.

[70] F. D'amélio, H. Vigerelli, Á. Rossan, B. Prieto-Da-Silva, E.O. Frare, I.D.F.C. Batista, D.C. Pimenta, I. Kerkis, Bothrops moojeni venom and its components strongly affect osteoclasts' maturation and protein patterns, Toxins 13 (2021), https://doi.org/10.3390/toxins13070459.

[71] R. Donne, F. Sangouard, S. Celton-Morizur, C. Desdouets, Hepatocyte polyploidy: driver or gatekeeper of chronic liver diseases, Cancers 13 (2021), https://doi.org/10.3390/cancers13205151.

[72] T. Matsumoto, Implications of polyploidy and ploidy alterations in hepatocytes in liver injuries and cancers, Int. J. Mol. Sci. 23 (2022), https://doi.org/10.3390/ijms23169409.

[73] Y. Miyaoka, K. Ebato, H. Kato, S. Arakawa, S. Shimizu, A. Miyajima, Hypertrophy and unconventional cell division of hepatocytes underlie liver regeneration, Curr. Biol. 22 (2012) 1166–1175, https://doi.org/10.1016/j.cub.2012.05.016.

[74] A. Schmidt, A. Hall, Guanine nucleotide exchange factors for Rho GTPases: turning on the switch, Genes Dev. 16 (2002) 1587–1609, https://doi.org/10.1101/gad.1003302.

[75] A. Bernards, GAPs galore! A survey of putative Ras superfamily GTPase activating proteins in man and Drosophila, Biochim. Biophys. Acta Rev. Canc 1603 (2003) 47–82, https://doi.org/10.1016/S0304-419X(02)00082-3.

[76] E. Dransart, B. Olofsson, J. Cherfils, RhoGDIs revisited: novel roles in Rho regulation, Traffic 6 (2005) 957–966, https://doi.org/10.1111/j.1600-0854.2005.00335.x.

[77] D. Spiering, L. Hodgson, Dynamics of the rho-family small GTPases in actin regulation and motility, Cell Adhes. Migrat. 5 (2011) 170–180, https://doi.org/10.4161/cam.5.2.14403.

[78] A.M. Gautreau, F.E. Fregoso, G. Simanov, R. Dominguez, Nucleation, stabilization, and disassembly of branched actin networks, Trends Cell Biol. 32 (2022) 421–432, https://doi.org/10.1016/j.tcb.2021.10.006.

[79] J. van Haren, T. Wittmann, Microtubule plus end dynamics – Do we know how microtubules grow?: cells boost microtubule growth by promoting distinct structural transitions at growing microtubule ends, Bioessays 41 (2019), e1800194, https://doi.org/10.1002/bies.201800194.

[80] A.J. Ridley, Rho GTPase signalling in cell migration, Curr. Opin. Cell Biol. 36 (2015) 103–112, https://doi.org/10.1016/j.ceb.2015.08.005.

[81] M.J.I. Paine, H.P. Desmond, R. David, G. Theakston, J.M. Crampton, Purification, cloning, and molecular characterization of a high molecular weight hemorrhagic metalloprotease, Jararhagin, from Bothrops jararaca venom - insights into the disintegrin gene family, J. Biol. Chem. 267 (1992) 22869–22876.

[82] E.P. Costa, C.B. Del Debbio, L.C. Cintra, L. da Fontoura Costa, D.E. Hamassaki, M.F. Santos, Jararhagin, a snake venom metalloprotease-disintegrin, activates the Rac1 GTPase and stimulates neurite outgrowth in neuroblastoma cells, Toxicon 52 (2008) 380–384, https://doi.org/10.1016/j.toxicon.2008.04.165.

[83] J. Pathan, A. Martin, R. Chowdhury, D. Chakrabarty, A. Sarkar, Russell's viper venom affects regulation of small GTPases and causes nuclear damage, Toxicon 108 (2015) 216–225, https://doi.org/10.1016/j.toxicon.2015.10.011.

[84] S.C. Sampaio, M.F. Santos, E.P. Costa, A.C. Rangel-Santos, S.M. Carneiro, R. Curi, Y. Cury, Crotoxin induces actin reorganization and inhibits tyrosine phosphorylation and activity of small GTPases in rat macrophages, Toxicon 47 (2006) 909–919, https://doi.org/10.1016/j.toxicon.2006.03.004.

[85] Y.W. Heng, C.G. Koh, Actin cytoskeleton dynamics and the cell division cycle, Int. J. Biochem. Cell Biol. 42 (2010) 1622–1633, https://doi.org/10.1016/j.biocel.2010.04.007.

[86] F.A. Urra, R. Araya-Maturana, Putting the brakes on tumorigenesis with snake venom toxins: new molecular insights for cancer drug discovery, Semin. Cancer Biol. 80 (2022) 195–204, https://doi.org/10.1016/j.semcancer.2020.05.006.

[87] M. Schnoor, C. Ugalde, Y. Samstag, E. Balta, J. Kramer, Redox regulation of the actin cytoskeleton in cell migration and adhesion: on the way to a spatiotemporal view, Front. Cell Dev. Biol. 1 (2021), 618261, https://doi.org/10.3389/fcell.2020.618261.

[88] R.K. Assoian, M.A. Schwartz, Integrins and RTKs in the regulation of G 1 phase cell-cycle progression, Curr. Opin. Genet. Dev. 11 (2001) 48–53.

[89] R.-M. Bohmer, E. Scharf, R.K. Assoian, Cytoskeletal integrity Is required throughout the mitogen stimulation phase of the cell cycle and mediates the anchorage-dependent expression of cyclin D1, Mol. Biol. Cell 7 (1996) 101–111.

[90] S. Huang, C.S. Chen, D.E. Ingber, Control of cyclin D1, p27 Kip1 , and cell cycle progression in human capillary endothelial cells by cell shape and cytoskeletal tension, Mol. Biol. Cell 9 (1998) 3179–3193.
[91] C. Margadant, A. van Opstal, J. Boonstra, Focal adhesion signaling and actin stress fibers are dispensable for progression through the ongoing cell cycle, J. Cell Sci. 120 (2007) 66–76, https://doi.org/10.1242/jcs.03301.
[92] C. Margadant, L. Cremers, A. Sonnenberg, J. Boonstra, MAPK uncouples cell cycle progression from cell spreading and cytoskeletal organization in cycling cells, Cell. Mol. Life Sci. 70 (2013) 293–307, https://doi.org/10.1007/s00018-012-1130-2.